LASER PROCESSING OF BIOLOGICAL MATERIALS

A Thesis
Presented to
The Academic Faculty

By

Timothy Patz

In Partial Fulfillment
Of the Requirements for the Degree
Masters of Science in Bioengineering

Georgia Institute of Technology
December 2005

LASER PROCESSING OF BIOLOGICAL MATERIALS

Approved by:

Dr. Roger J. Narayan, M.D. Ph.D., Advisor
School of Material Science & Engineering
Georgia Institute of Technology

Dr. Ravi Bellamkonda, Ph.D.
Department of Biomedical Engineering
Georgia Institute of Technology

Dr. Barbara Boyan, Ph.D.
Department of Biomedical Engineering
Georgia Institute of Technology

Date Approved: June 10th, 2005

ACKNOWLEDGEMENT

First, I would like to thank my advisor Dr. Roger Narayan, Dr. Chunming Jin, and Andy Doraiswamy for their support with my research. Second, I would like to thank the Bellamkonda group, including Dr. Ravi Bellamkonda, Wei He and Yinghui Zhong. Third, I would like to thank the efforts of Nick Menegazzo, Christine Kranz and Boris Mazaikoff for their work regarding FTIR and AFM. Finally, I would like to thank my family for their support: my mother Rosanna, my father Fredrick, my brother Dan and my fiancée Yau-Ru.

TABLE OF CONTENTS

Acknowledgements iii

List of Figures vi

List of Symbols or Abbreviations ix

Summary x

Chapter 1. Introduction 1

1.1 Background 1

1.2 Matrix assisted pulsed laser evaporation (MAPLE) 2

1.3 Matrix assisted pulsed laser evaporation direct write (MDW) 6

Chapter 2. MAPLE Deposition of PDLLA/Dexamethasone Bilayers 10

2.1 Introduction 10

2.2 Materials and methods 13

2.2.1 Material Sourcing 13

2.2.2 Matrix Assisted Pulsed Laser Evaporation 13

2.2.3 Fourier Transform Infrared Spectroscopy 14

2.2.4 X-ray Photoelectron Spectroscopy 15

2.2.5 Atomic Force Microscopy 15

2.2.6 Attenuated Total Reflection Fourier Transform Infrared Spectroscopy 15

2.2.7 Microglia Cultures and Nitric Oxide Production 16

2.2.8 UV Spectrophotometry Dexamethasone Release 17

2.3 Results and discussion 17

Chapter 3. MDW Three-Dimensional Deposition of Neuroblasts 27

3.1 Introduction 27

3.2 Materials and methods 30

3.2.1 Matrix Assisted Pulsed Laser Evaporation Direct Write 30

3.2.2 Neuronal Culture and MDW Ribbon Creation 31

3.2.3 Receiving Substrate 31

3.2.4 Apoptosis Detection via TUNEL Staining 32

3.2.5 Characterization of Neuronal Morphology in the 3-D ECM Gel 33

3.2.6 Live/Dead Assay 33

3.3 Results and discussion 34

Chapter 4. Conclusions and future directions 43

References 47

LIST OF FIGURES

Figure 1	A comparison of the overlapping characteristics of physical vapor deposition, solvent casting/coating and MAPLE.	3
Figure 2	Schematic of the MAPLE deposition process.	5
Figure 3	Schematic of the LIFT process.	6
Figure 4	Schematic of the MAPLE Direct Write process.	8
Figure 5	PDLLA chemical structure.	11
Figure 6	Chemical structure of dexamethasone.	12
Figure 7	Fourier transform infrared spectra of dropcast and matrix assisted pulsed laser evaporation-deposited PDLLA thin films. The spectra were recorded in transmission mode.	18
Figure 8	C1s X-ray photoelectron spectrum of PDLLA, revealing peaks at 285, 287 and 289 eV. These peaks correspond to C-H, C-O and C=O, which correspond to 38.4, 30.1 and 31.4% of the total C1s area, respectively.	19
Figure 9	O1s X-ray photoelectron spectrum of PDLLA. The O1s component at 532.6 eV and 534.1 eV correspond to O=C and O-C bonding, and represent 52 and 48 % of the total O1s area, respectively.	19
Figure 10	Topography flattened atomic force micrograph of a MAPLE deposited PDLLA thin film (a), with a height profile (b).	20
Figure 11	Topography flattened atomic force micrograph of MAPLE deposited dexamethasone thin film (a) and height profile (b).	21
Figure 12	Deflection flattened atomic force micrograph of the MAPLE dexamethasone thin film.	22
Figure 13	ATR-IR spectra of dexamethasone deposited on Si wafers by (A) drop casting, and (B) MAPLE.	23
Figure 14	Effect of dexamethasone released from PDLLA/dexamethasone thin films. Microglia were treated with LPS and dexamethasone was released for 48 hours, inhibiting LPS-induced production of nitrite. Cells without LPS treatment served as positive	

control. Microglia subjected to LPS serum served as a negative control. Data shown are the average ± S.E.M. (n=3). *$P < 0.05$ compared with LPS-treated cultures. 24

Figure 15 Mass release of dexamethasone from MAPLE deposited PDLLA-dexamethasone bilayer. Data shown is average ± S.E.M. (n=3). 25

Figure 16 Cumulative mass of dexamethasone released from MAPLE deposited PDLLA-dexamethasone bilayers. Data shown is average ± S.E.M. (n=3). The release profile can be predicted by a logarithmic function at $R^2 = 0.9951$. 26

Figure 17 TUNEL staining of transferred B35 neuroblasts. The cells were fixed 96 hours after laser transfer. All cell nuclei counterstained with DAPI nucleic acid stain (blue). No DNA breakage is observed (red). 35

Figure 18 Number of axonal projections over time for MDW-transferred and control neuroblasts. Each bar represents mean ± STD. Using a students t-test, we found that $p > 0.05$, showing that the MDW transferred neuroblast data was similar to control. 36

Figure 19 Percentage of live neuroblasts deposited by MDW vs. control. Each bar represents mean ± STD. Using a students t-test, we found that $p > 0.05$, proving that the MDW transferred neuroblast data was similar to control. 36

Figure 20 (a) Two-dimensional optical micrograph of B35 neuroblast patterns 24 hours after MDW transfer. The deposited neuroblasts can be seen extending axons over the two-dimensional plane of the extracellular matrix surface. (b) Two-dimensional optical micrograph of B35 neuroblast patterns 72 hours after MDW transfer. The neuroblasts have extended their axons to form local neural networks. 38

Figure 21 Confocal micrograph of the B35 neuroblasts 75 μm below the extracellular matrix surface 24 hours after MDW transfer. The neuroblasts have extended their axons throughout the three-dimensional ECM network. 39

Figure 22 Confocal micrograph of transferred B35 neuroblasts within the extracellular matrix. Axonal extensions were observed between neuroblasts on different deposition planes, which were spaced 30-40 μm apart. 40

Figure 23 Neuroblast penetration depth (μm) vs. applied laser fluence (J/cm^2). The non-linear effect of applied laser fluence on neuroblast penetration depth is clearly observed. 41

LIST OF SYMBOLS or ABBREVIATIONS

MAPLE – matrix assisted pulsed laser evaporation

PVD – physical vapor deposition

MDW – matrix assisted pulsed laser evaporation direct write

LIFT – laser induced forward transfer

CAD/CAM – computer aided drafting / computer aided machining

UV – ultraviolet

PDLLA – poly-d, l lactide

FTIR - Fourier transform infrared spectroscopy

XPS – x-ray photoelectron spectroscopy

AFM – atomic force microscopy

PBS – phosphate buffer solution

DMEM – Dulbecco's modified eagle medium

ECM – extracellular matrix solution

SUMMARY

I have explored the use of the matrix assisted pulsed laser evaporation (MAPLE) and MAPLE direct write (MDW) to create thin films of biological materials. MAPLE is a novel physical vapor deposition technique used to deposit thin films of organic materials. The MAPLE process involves the laser desorption of a frozen dilute solution (1-5%) containing the material to be deposited. A focused laser pulse (~200 mJ/cm2) impacts the frozen target, which causes the solvent to preferentially absorb the laser energy and evaporate. The collective action of the evaporated solvent desorbs the polymeric solute material towards the receiving substrate placed parallel and opposite to the target. The bioresorbable polymer PDLLA and the anti-inflammatory pharmaceutical dexamethasone were processed using MAPLE, and characterized using Fourier transform infrared spectroscopy, atomic force microscopy and x-ray photoelectron spectroscopy. MDW is a CAD/CAM controlled direct writing process. The material to be transferred is immersed in a laser-absorbing matrix or solution and coated onto a target or support positioned microns to millimeters away from a receiving substrate. Using a UV microscope objective, a focused laser pulse is directed at the backside of the ribbon, so that the laser energy first interacts with the matrix at the ribbon/matrix interface. This energy is used to gently desorb the depositing material and matrix onto the receiving substrate. I have deposited neuroblasts within a three-dimensional extracellular matrix sheet (~75μm). These two laser processing techniques have enormous potential for functional medical device and tissue engineering applications.

Chapter 1. Introduction

1.1 Background

Since their invention in the early 1960s, lasers have had many uses in the medical field. Lasers are ideal for removing unwanted tissue, because they are able to direct high energy radiation of a single wavelength onto a focused location. Most current medical uses of lasers fall under the use of the laser as a "universal scalpel" in minimally invasive surgeries, which offer little contact, little blood loss, shorter operating times, and less postoperative pain than conventional techniques. Laser in situ keratomileusis (LASIK) refractive corneal surgery, coagulation for retinal detachment, and skin treatments are only some of the current applications for lasers in medicine. Lasers-tissue interaction may also provide a characteristic luminescence that is useful in sensing blood flow, oxygen concentration, and pH within tissue.

In the future, lasers may serve to create novel medical devices with unique biological functionalities. For example, lasers offer a unique opportunity for nanoscale processing of materials. Nanostructured biosensors, drug delivery devices, tissue scaffolds, and membranes may provide the capability for specific interactions with proteins, DNA, viruses, and other biological structures. In this manuscript, I will discuss the current status of the laser processing methods: matrix assisted pulsed laser evaporation (MAPLE) and matrix assisted pulsed laser evaporation direct write (MDW), for the development of drug delivery thin films, and cells deposited three-dimensionally within extracellular matrices.

1.2 Matrix Assisted Pulsed Laser Evaporation (MAPLE)

Today, there is a great need for depositing high quality organic and polymer thin films, multilayers, and composites. Moreover, there is a need for a method that can maintain strict tolerances on the structural, morphological, and chemical composition of the film. For example, in biological and chemical sensor applications, high quality thin films of chemoselective or bioselective materials must be processed so that the physiochemical properties are maintained. Current implantable medical devices, such as artificial hip prosthesis, catheters, and pacemakers typically need to be coated with a passivation layer to protect the devices from interaction with bodily fluid that may cause corrosion or degradation. Next generation medical devices will likely contain multi-layer coatings along with some type of pharmacological agent or growth factor. Possible coating materials for such an application may be synthetic (poly D, L lactide) or natural (chitosan) polymers. In both cases, these films must be processed by a technique that will not damage the materials, and allow strict control of the film characteristics.

To fully exploit the bulk properties of natural and synthetic polymers, the thin film must mimic these attributes. Physical vapor deposition (PVD) techniques that successfully deposit more robust materials such as metals will not work because the organic or polymer material is too fragile for this process. Solvent-based coating technologies, such as spin-coating, dip-coating and drop-casting, typically result in inhomogeneous films with difficult thickness control and are restricted to single layers. However, some attributes of PVD processes would be highly beneficial in depositing high quality organic and polymeric thin films. For instance, layer-by-layer growth, control thickness, clean interfaces, and dry processing in PVD and material salvation in

solvent coating techniques would be ideal attributes of an organic or polymer thin film deposition technique. Matrix assisted pulsed laser evaporation (MAPLE) is a thin film deposition technique, which uses aspect from both PVD and solvent coating techniques. A diagram explaining the overlapping of these three techniques is shown in Figure 1.

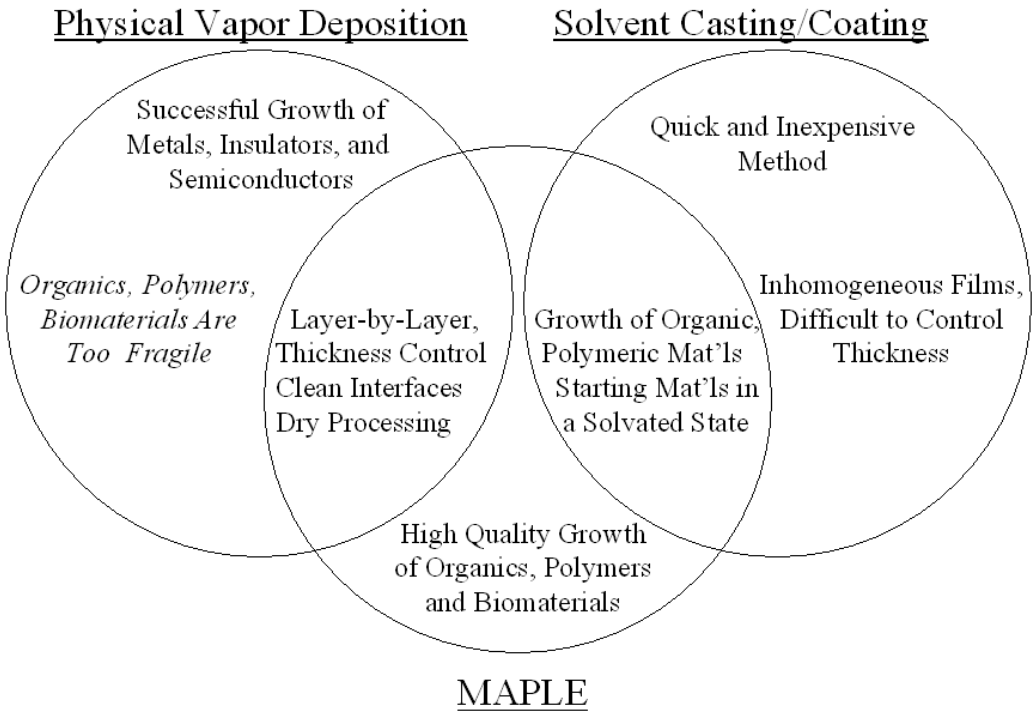

Figure 1. A comparison of the overlapping characteristics of physical vapor deposition, solvent casting/coating and MAPLE.

MAPLE is a novel physical vapor deposition technique used to deposit thin films of polymeric, biologic, pharmacologic and other fragile organic materials onto a substrate. [1,2] A schematic diagram of the MAPLE deposition process is shown in Figure 2. The MAPLE process involves the laser desorption of a frozen dilute solution (1-5%) containing the material to be deposited. The laser-material interaction in MAPLE has been described as a photothermal process. [1] A focused laser pulse (~200 mJ/cm^2) impacts the frozen target, and the photon energy absorbed by the solvent is converted into

thermal energy, causing the solvent to evaporate. As the surface solvent molecules are vaporized, polymer molecules become exposed to the gas-target matrix interface. Through collisions with the evaporating solvent molecules, the polymer molecules attain enough kinetic energy to be transferred into the gas phase. The collective action of the evaporated solvent desorbs the polymeric solute material towards the receiving substrate placed parallel and opposite to the target. As deposition takes place in a vacuum chamber onto a room temperature substrate, the evaporated volatile solvent is not absorbed in the film and rapidly pumped away. Through careful optimization of MAPLE deposition conditions, deposition can occur without any significant polymer decomposition, e.g., for polymers this means minimal to no reduction in the degree of polymerization chemical modification or loss of functional groups. [1] The MAPLE process proceeds layer-by-layer, depleting solvent and polymer in the same concentration as the starting solution. The advantage of MAPLE is that it has the important attributes of a dry physical vapor deposition technique like sputtering or e-beam evaporation, yet it handles the fragile material in a solvated state.

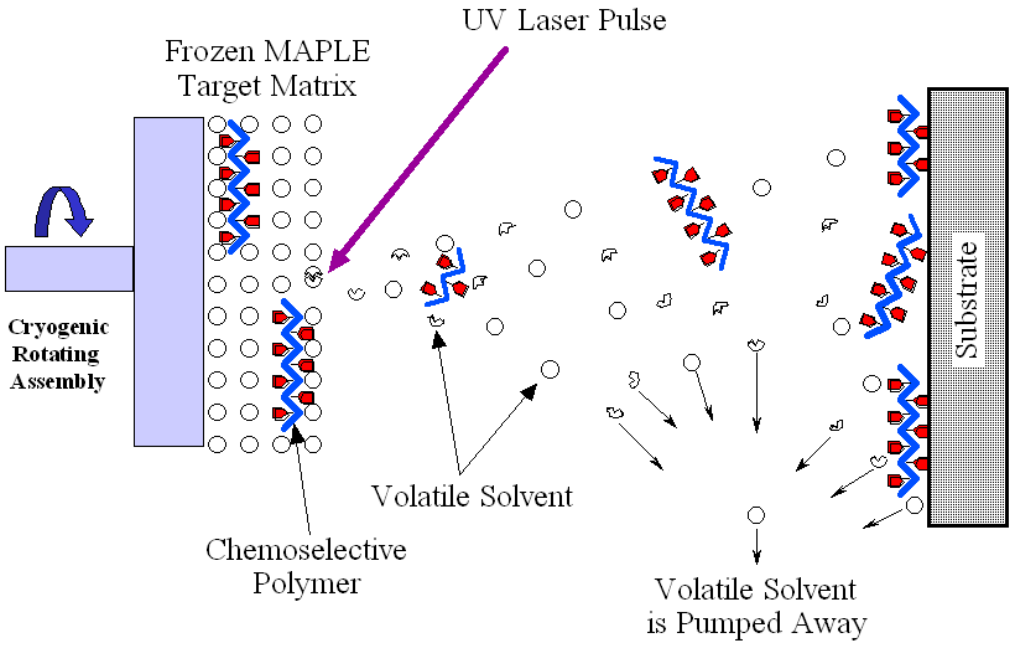

Figure 2. Schematic of the MAPLE deposition process

One of the original applications for the MAPLE technique was the deposition of thin, homogenous films of a chemoselective polymer used on sensing platforms such as surface acoustic wave devices.[3] Since this initial experiment, MAPLE has been used to deposit a wide range of organics and polymers. Various carbohydrates, such as sucrose, glucose and dextran have been deposited. [4] Biocompatible polymers thin films of polyethylene glycol (PEG) have also been successfully deposited. [5] More recently, the need has developed for the growth of biomaterial thin films for the development of next-generation biosensors or biochips, drug delivery, and coatings for medical devices. Deriving from this need, fragile organic thin films of horseradish peroxidase [6], type I collagen [7], bovine serum albumin and phospholipid polymers [8] have been produced using MAPLE.

1.3 Matrix Assisted Pulsed Laser Evaporation Direct Write (MDW)

Direct writing is a powerful approach to fabricate patterns of material that are completely CAD/CAM controlled and do not rely on various masks or molds. Derived from the need to rapid construct electronic devices, many different direct writing techniques were first used to direct write passive electronics. Of these processes, laser forward transfer is one approach that is especially flexible because: optical imaging is built into the system, transfer is possible for any material, and this technique can rapidly fabricate as well as provide laser annealing, cleaning, and micro machining. Although lasers are not typically associated with construction of materials, they can be a gentle method to transfer and process materials.

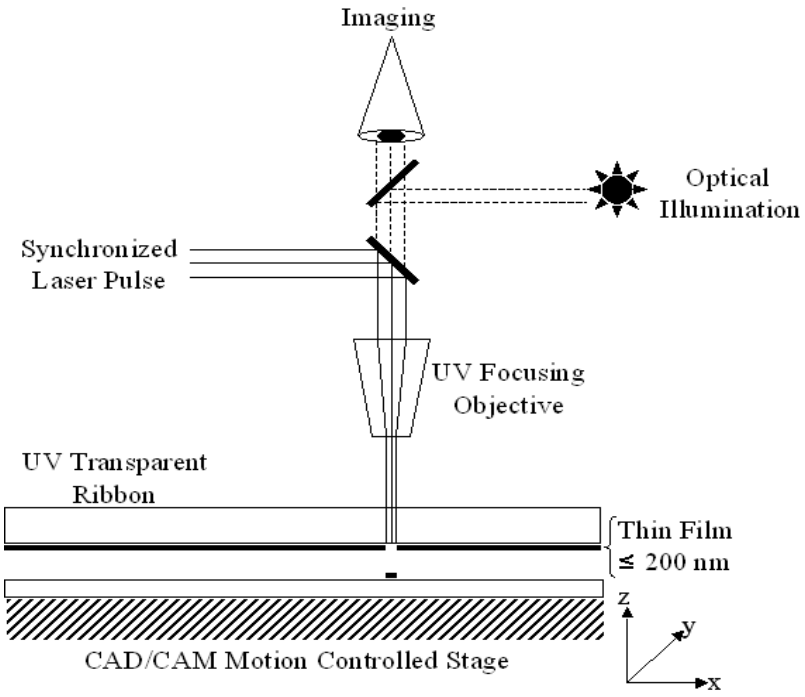

Figure 3. Schematic of the LIFT process.

Laser induced forward transfer (LIFT) is a very simple approach to direct writing materials (Figure 3). The LIFT technique requires a thin film (about 200 nm) deposited

onto a laser transparent support to be pressed slightly to a receiving substrate. [9] Pulsed laser shots pass through the laser transparent support to atomize the thin film on the opposite side and deposit the coated material onto the receiving substrate. Originally, this method was successful in depositing metal [10,11] and inorganic [12] thin films; however, the design setup had to be slightly modified to extend the capabilities of the LIFT process to transfer a wider range of materials and at a higher deposition rate. A schematically similar technique to LIFT, termed matrix assisted pulsed laser evaporation direct write (MDW), was developed to more gently deposit materials without excessive heating of the surrounding material.

MDW is a CAD/CAM controlled direct writing process that is schematically similar to LIFT because the material to be transferred is immersed in a laser-adsorbing matrix or solution and coated onto a target or support. However, in MDW, the transfer support, or "ribbon," is not coated with a metal absorbing layer and it is positioned microns to millimeters away from a receiving substrate. Using a UV microscope objective, a focused laser pulse is directed at the backside of the ribbon, so that the laser energy first interacts with the matrix at the ribbon/matrix interface. This energy is used to gently desorb the depositing material and matrix onto the receiving substrate. To deposit patterns, a computer program controls the motion of an X-Y transition stage, which controls the lateral and longitudinal movement of both the ribbon and receiving substrate. A schematic of the MDW apparatus is shown in Figure 4.

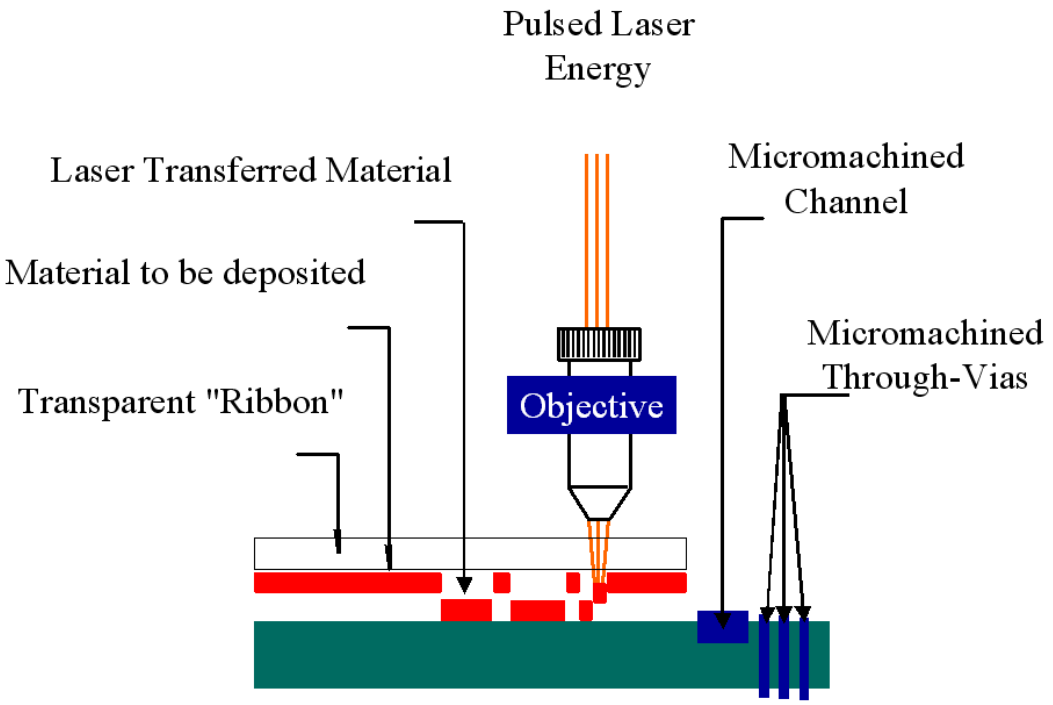

Figure 4. Schematic of the MAPLE Direct Write process.

MDW was originally designed as a method to rapidly construct electronic devices such as interconnects, resistors, and capacitors. [13,14] MDW has been used to deposit metals, ceramic powders, nano-powders, and organometallic precursors using an experimental set-up similar to LIFT, but by coating the transparent ribbon with solvated materials it was mechanistically different. The laser-solvent material interaction resulted in a matrix-assisted transfer similar to the vacuum MAPLE process. [15] MDW was able to transfer organic and polymeric materials for the fabrication of gas sensor chemi-resistors [13] and chemical sensors [16]. MDW was also used as a fabrication method to deposit more sensitive materials such as proteins and living cells for the construction of protein microarrays [17] and tissue based sensors. [8] In 2001, Ringeisen et al. were able to transfer viable Chinese hamster ovaries. [6] MDW has also had success depositing embryonal carcinoma [18], rat cardiac [1], and human osteoblast cells. [8]

In MDW, the UV laser irradiation must be totally attenuated in the solvent otherwise the radiation may genetically alter the cells. It is well known that UV irradiation of biological materials can be irreversibly destructive causing DNA damage. Any processing technique used in a medical setting should not create new health problems in an attempt to eliminate others. Preliminary mutagenicity studies have fortunately shown no evidence of DNA strand breakage. An initial neutral comet assay on transferred p19 cells found no evidence of double strand breaks. [18] In my research, a follow up comet assay also showed that transferred neuroblasts did not undergo apoptotic DNA double strand breaks. It is possible that cytoplasmic proteins within the media matrix absorb the laser radiation, and protect the DNA.

Chapter 2. MAPLE Deposition of PDLLA/Dexamethasone Bilayers

2.1 Introduction

It has been estimated that at least 40 million people worldwide suffer from epilepsy and 1 in 20 people will have an epileptic seizure. [19] Epilepsy is a brain disorder in which clusters of neurons in the brain signal abnormally. This disruption of electrical signals in the brain leads to seizures. However, once epilepsy is diagnosed, seizures can be controlled with medicine and monitored with surgical techniques such as electroencephalography.

Electroencephalography, or EEG, is a neurological test that uses an electrical monitoring device to measure electrical activity in the brain. EEG is a key tool in the diagnosis and management of epilepsy and other seizure disorders. [20] It is also used as a diagnostic tool for patients suffering from mental retardation, sleep disorders and various degenerative diseases such as Alzheimer's disease. [21] For a patient undergoing EEG, electrodes can be attached to the patients scalp; however, depending on the purpose for the EEG, implantable or invasive electrodes are necessary. One significant drawback of using invasive electrodes, which are surgically inserted into the brain, is the risk of scarring. [22]

Any neural implants inserted into the brain cause tissue injury, which initiates a series of cellular and molecular events. [23] Histological evidence shows that a cellular sheath surrounds the insertion site of Si microelectrodes, which is a typical consequence of inflammatory reaction resulting from physical injury to the central nervous system (CNS). [24] In the CNS, this process of sheath formation is termed "reactive gliosis" or astroglial scarring. The glial scar forms an inhibitory barrier preventing axon re-growth

and functions as a diffusive barrier that is thought to reduce the ability of implanted devices to communicate with neurons by insulating the device from the surrounding brain tissue. [25] To maintain long-term recording stability, reactive gliosis and other inflammatory processes around the electrode need to be minimized [26].

We propose a novel method of neuronal implant drug coating, which involves using MAPLE to coat the implant with single or multiple bilayers of a biodegradable polymer covering an inflammatory pharmaceutical. Depositing a uniform polymer/drug thin film multilayer coating onto the implant surface would slow the absorption of the drug thereby delivering a more sustained anti-inflammatory pharmaceutical dosage.

Poly D, L lactide or PDLLA is a polymer derived from the optically active D and L monomers of PLA. The chemical structure of this biodegradable polyester is shown in Figure 5. PDLLA degrades faster than PLA, the homopolymer of L-lactic acid, because it is amorphous. Since PDLLA is amorphous, it is more likely to exhibit a homogeneous dispersion of the active species within a monophasic matrix. PDLLA degradation occurs via chain scission, during which polymer chains are cleaved to form oligomers and then monomers. The erosion process can be described as the loss of oligomers and monomers leaving the polymer film. Degradation of these lactide based polymers and other hydrolytically degradable polymers depend on chemical composition crystallinity, and hydrophilicity.

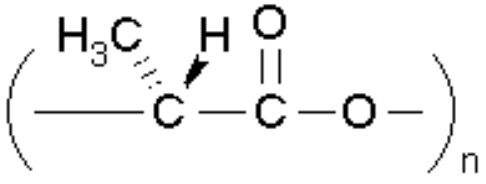

Figure 5. PDLLA chemical structure.

Dexamethasone is in the class of drugs known as glucocorticoids, which are known to inhibit cellular inflammation processes as well as prevent smooth muscle cell proliferation and collagen formation. [27] Glucocorticoids inhibit some of the mechanisms involved in cell-mediated immunologic functions, especially those dependent on lymphocytes. They also have a dramatic effect on the distribution and function of leukocytes. Specifically, dexamethasone is known to regulate T-cell survival, growth and differentiation. As a locally delivered therapeutic, dexamethasone is an ideal drug coating for use on medical implants. Local delivery is also advantageous because systematic exposure to glucocorticoids can result in toxicity including adrenal suppression, metabolic effects (growth inhibition, diabetes, and osteoporosis), salt retention, and psychosis. [27] The chemical structure of dexamethasone is shown in figure 6.

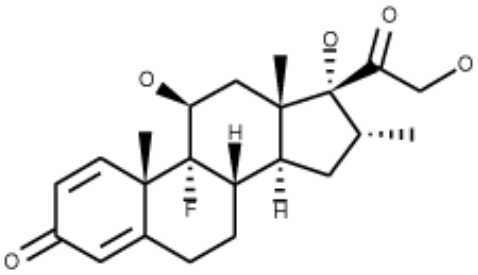

Figure 6. Chemical structure of dexamethasone.

Following neural electrode insertion, microglia mediate the initial inflammatory response to brain injury. Microglia produce inflammatory molecules such as nitric oxide, IL-1β, TNF α, which induce neuronal cell death and trigger the activation of astrocytes, which finally result in glial scar formation. [28-30] Dexamethasone is a corticosteroid

with potent anti-inflammatory properties, which has been widely used clinically for treatment of inflammation or immune response as well as chronic inflammatory disorders. Most importantly, dexamethasone has been previously shown to inhibit microglia proliferation, NO production, and cytokine secretion. [31]

We have demonstrated successful deposition of PDLLA thin films on ZnSe substrates and PDLLA/dexamethasone bilayer films on SiO_2. Using Fourier transform infrared spectroscopy, atomic force microscopy, and X-ray photoelectron spectroscopy, we have shown that our PDLLA/dexamethasone films were deposited with micro-scale smoothness and maintained their chemical structure post-transfer. Additionally, we have also shown that dexamethasone maintained its bioactivity post transfer.

2.2 Materials and Methods

2.2.1 Material Sourcing

PDLLA was commercially obtained (Sigma Aldrich, St. Louis, MO). The manufacturer's listed molecular weight is 75,000-120,000. To create a suitable MAPLE target matrix, the PDLLA was solvated into a 4% g/ml solution with ethyl acetate (Fisher Scientific, Hampton, NH). Dexamethasone (Sigma Aldrich, St. Louis, MO) was solvated into 2% g/ml solution using ethyl acetate. The manufacturor's listed molecular weight for dexamethasone is 392.46.

2.2.2 Matrix Assisted Pulsed Laser Evaporation

MAPLE depositions of each material were performed using a pulsed Lambda Physik ArF laser (λ=193 nm, τ_{FWHM}=30 ns, pulse rate=20 Hz, laser fluence=600-1000 mJ/cm^2). The incident angle of the laser beam was placed at an angle of 45^o with respect

to the normal of the target surface. The target-substrate distance was maintained at 70 mm, and the spot area was maintained between 2.5-3.5 mm^2. Prior to deposition, ~1 ml of the solvated fluid was pipetted into the target holder and frozen using liquid nitrogen. The aluminum target holder was placed on a cryogenic rotating assembly, which was maintained at a temperature of ~ 173 K using copper braids connected to a liquid nitrogen reservoir. The MAPLE chamber is then evacuated to a pressure of 10^{-4} Pa. Some of the samples were run with nitrogen gas purge into the sample chamber. The target was rotated at a rate of 0.4 Hz during film deposition. As a control, films were also prepared by drop casting in order to provide comparison data.

For the deposition of the PDLLA/dexamethasone bilayer, we first deposited a layer of dexamethasone using 100,000 laser pulses and then deposited a layer of PDLLA using 40,000 laser shots. The fluence for each material was maintained at 700 mJ/cm^2. PDLLA and dexamethasone thin films were also prepared by drop casting in order to provide comparison data.

2.2.3 Fourier Transform Infrared Spectroscopy

Fourier transform infrared spectroscopy (FTIR) was used to analyze the bending and stretching of the chemical bonds within the PDLLA thin film, and to insure that no structural damage occurred during material transfer. 100 averaged scans were taken from a Bruker IFS/66 spectrometer with a 4 cm^{-1} resolution. Each PDLLA MAPLE sample was deposited on ZnSe crystal, and, therefore, the background spectrum was taken on uncoated ZnSe. The sample compartment was purged with dry air for at least 25 minutes prior to data recording to reduce the contribution of water vapor and carbon dioxide to

the resulting spectrum. The measurements were taken in transmission mode, and the range recorded was 4000-600 cm^{-1}.

2.2.4 X-ray Photoelectron Spectroscopy

X-ray photoelectron spectroscopy data was acquired using a Surface Science Laboratories Model SSX-100 Small Spot ESCA Spectrometer containing a monochromatized Al K-alpha X-ray source. A SPI Model 9602 True Spot electron gun was used to help control specimen charging. Spectra were collected at a 400-800 μm diameter X-ray spot size using a spectrometer pass energy of 50-150 eV. PDLLA C1s and O1s spectra were recorded.

2.2.5 Atomic Force Microscopy

Atomic force microscopy (AFM) experiments were performed to investigate the surface morphology of the polymer and drug thin films. All measurements were obtained with a PicoPlus atomic force microscope (Molecular Imaging, Tempe, AZ, USA) equipped with a scanning head providing a maximum scan range of 100 x 100 μm. Imaging was performed in contact mode using silicon nitride cantilevers (length: 200 μm; nominal spring constant: 0.06 Nm-1) with integrated pyramidal tips (base: 4x4 μm2; height: 2.86 μm). The imaging rate was 1.5 Hz.

2.2.6 Attenuated Total Reflection Fourier Transform Infrared Spectroscopy

To characterize the chemical composition of dexamethasone deposited by MAPLE, attenuated total reflection Fourier transform infrared spectroscopy (ATR-FTIR) was performed using a IR100 spectrometer (Thermal Electron Corporation, San Diego, CA). The samples were scanned 32 times in the range of 2000 to 1200 cm^{-1}. ATR-FTIR was performed on dexamethasone deposited substrates either by solvent casting or by

MAPLE deposition to determine if MAPLE deposition would alter the chemical structure of the drug.

2.2.7 Microglia Cultures and Nitric Oxide Production

Microglia were isolated from mixed primary glial cell cultures. Cells dissociated from neonatal Sprague-Dawley rat cerebral hemispheres were plated in 75 cm^2 poly-L-lysine coated tissue culture flasks (Fisher Scientific, Hampton, NH) at a density of one brain per flask in culture medium consisting of DMEM-F12 media (Invitrogen, Carlsbad, CA) supplemented with 20% fetal bovine serum and 1% penicillin/streptomycin. After 7-10 days, flasks were lightly shaken to release microglial cells into the media supernatant, and the floating microglia were subsequently spun down, and resuspended in DMEM-F12 media supplemented with 10% fetal bovine serum. The cells were seeded in 96-well culture plates at a density of 3×10^4 cells per well. Twenty-four hours after seeding, microglial cells were treated with 10-pg/ml lipopolysacchride (LPS) (Sigma Aldrich, St. Louis, MO) and the released dexamethasone diluted to a concentration of 0.5 μg/ml for 48 hours.

Nitric oxide (NO) production by the microglial cultures was determined by measuring the accumulated levels of nitrite in the supernatant with Griess reagent (Promega, Madison, WI). Briefly, after stimulation with LPS for 48 h, 50 μl cell culture supernatant was incubated with 50 μl sulphanilamide and 50 μl NED for 10 min each at room temperature. The optical density was measured at 540 nm using a microplate reader (Bio-Tek Instruments, Winooski, VT). NO production with and without dexamethasone when activated by LPS was determined.

2.2.8 UV Spectrophotometry Dexamethasone Release

PDLLA/dexamethasone bilayers were deposited on Si (100) wafers using MAPLE. Following deposition, the PDLLA/dexamethasone bilayers were incubated in phosphate buffer solution (PBS) at 37°C. Every 24 hours, the PBS was removed and replaced with fresh PBS. The amount of dexamethasone released during each 24 h period was measured by UV spectrophotometry at 242 nm with a microplate reader.

2.3 Results and Discussion

Figure 7 compares the PDLLA FTIR spectra from the drop cast sample and a representative MAPLE thin film. The drop cast and MAPLE films share numerous absorption peaks over the entire spectra. More importantly, they share similar absorbance at the main absorption sites: 1095 cm^{-1}(symmetric stretching of COC bond), 1758 cm^{-1} (stretching of C=O bond), and 2994 and 2944 cm^{-1} (stretching of the CH_3 groups). [32]

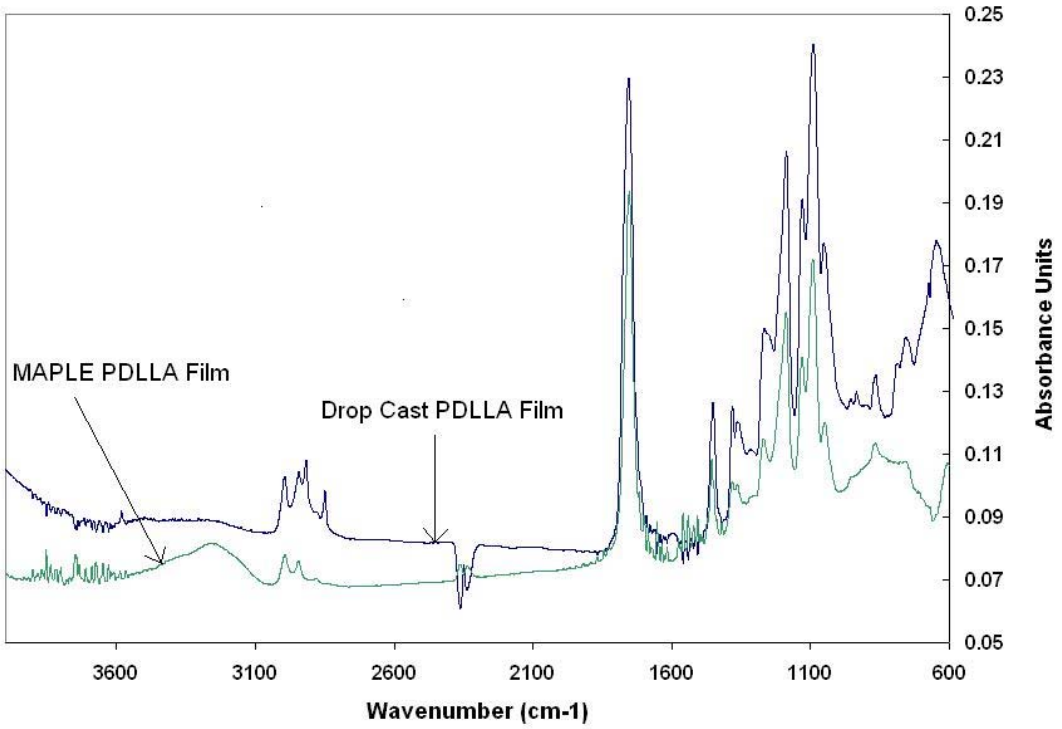

Figure 7. Fourier transform infrared spectra of dropcast and matrix assisted pulsed laser evaporation-deposited PDLLA thin films. The spectra were recorded in transmission mode.

The XPS C1s spectrum of PDLLA is made up of C-H groups, C-O groups in ester linkages and C=O groups in ester linkages at approximately 285, 287 and 289 eV, respectively. [33] In the MAPLE deposited PDLLA C1s XPS spectrum (Figure 8), the carbon concentrations of the C-H, C-O and C=O bonds, have been estimated by integrating the peak areas and represent 38.4, 30.1 and 31.4% of the C1s spectrum, respectively. The concentrations seen in our PDLLA film are similar to those obtained in previous PDLLA XPS analysis. [34-5] For the O1s PDLLA spectra shown in figure 9, the absorption peak is broken up into two components. The O1s component at 532.6 eV corresponds to O=C bonding, while the peak at 534.1 eV represent O-C groups. The concentrations for the O=C and O-C components are 52 and 48 %, which is close to the

ideal 1:1 ratio. Again, the peak positions and concentrations are similar to previously published data. [34-5]

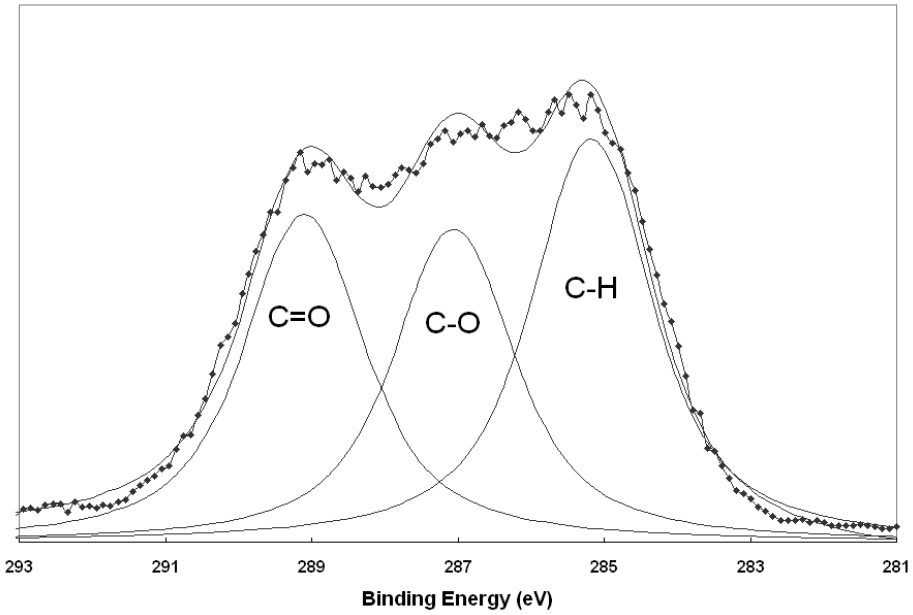

Figure 8. C1s X-ray photoelectron spectrum of PDLLA, revealing peaks at 285, 287 and 289 eV. These peaks correspond to C-H, C-O and C=O, which correspond to 38.4, 30.1 and 31.4% of the total C1s area, respectively.

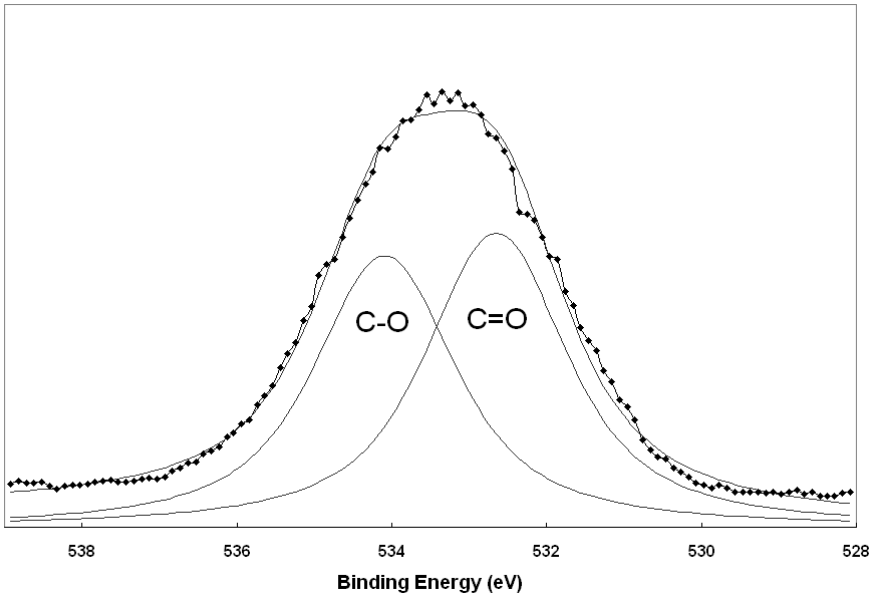

Figure 9. O1s X-ray photoelectron spectrum of PDLLA. The O1s component at 532.6 eV and 534.1 eV correspond to O=C and O-C bonding, and represent 52 and 48 % of the total O1s area, respectively.

Figure 10 contains an atomic force micrograph of a PDLLA thin film prepared by MAPLE (laser fluence= 1 J/cm^2). Inset (b) contains a plot of the height profile. Over the 17 microns covered, the thin film height varied nearly 400 nm. This sample, similar to the other PDLLA thin films, contained random height differentials between 200-600 nm. These small height differences can be associated to the random dispersing of desorbed polymer from the MAPLE target. A similar result was seen with the deposition of horseradish peroxidase via MAPLE where thin films maintained an average roughness of 200 nm. [6]

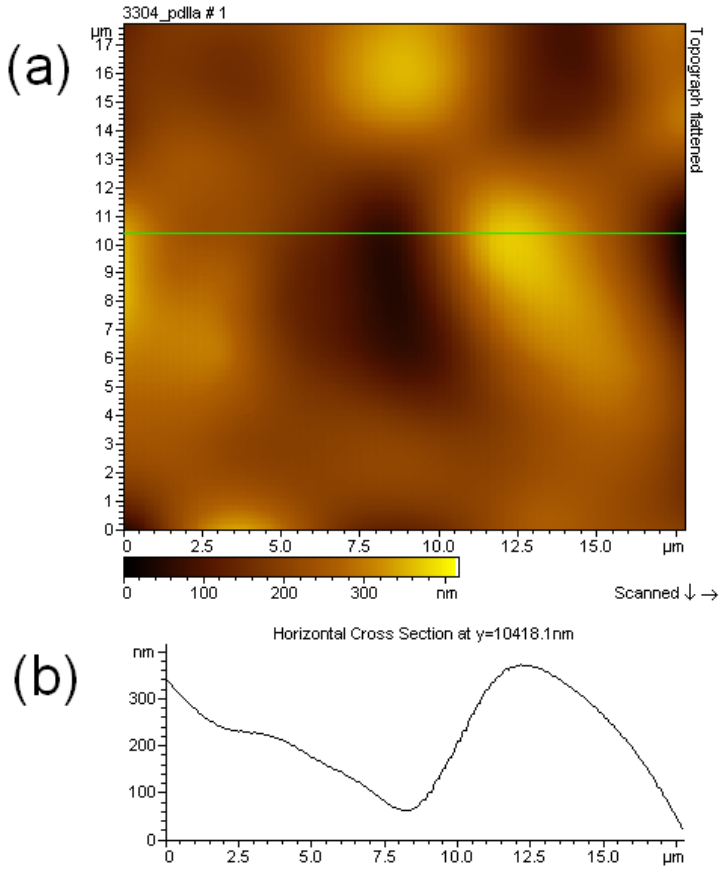

Figure 10. Topography flattened atomic force micrograph of a MAPLE deposited PDLLA thin film (a), with a height profile (b).

A topography flattened AFM image of a dexamethasone coated MAPLE film is shown in Figure 11. Inset (b) contains a plot of the height profile. Unlike the PDLLA films, dexamethasone has a unique surface topography. Ring-like structures 2-10 μm in length are observed. These structures are better observed in the deflection flattened AFM micrograph (Figure 12) of the dexamethasone thin film seen in Figure 11. These structures are caused by projection of small particles of the dexamethasone from the MAPLE target onto the substrate. This phenomenon, known as target splashing, is similar to an effect seen in pulsed laser deposition. [36]

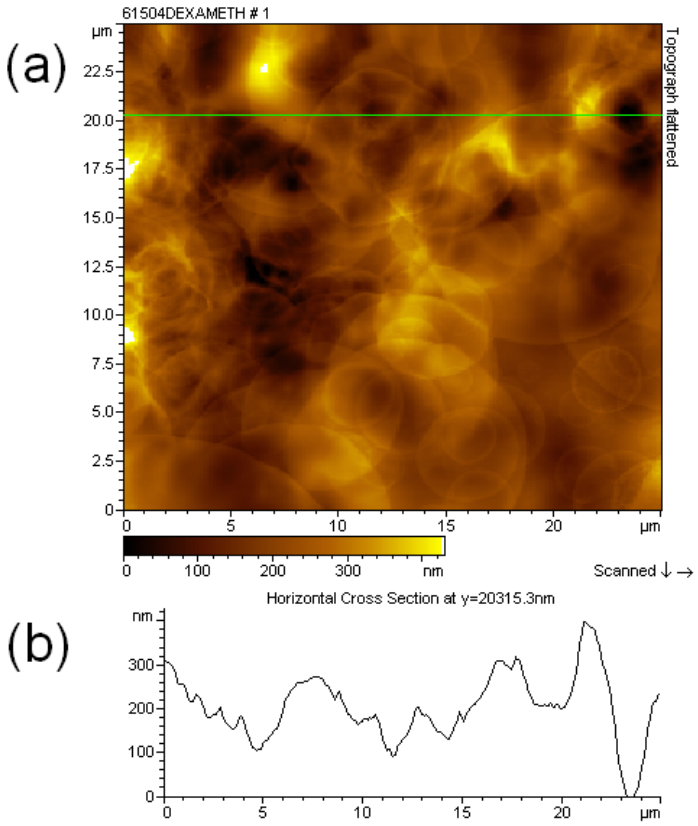

Figure 11. Topography flattened atomic force micrograph of MAPLE deposited dexamethasone thin film (a) and height profile (b).

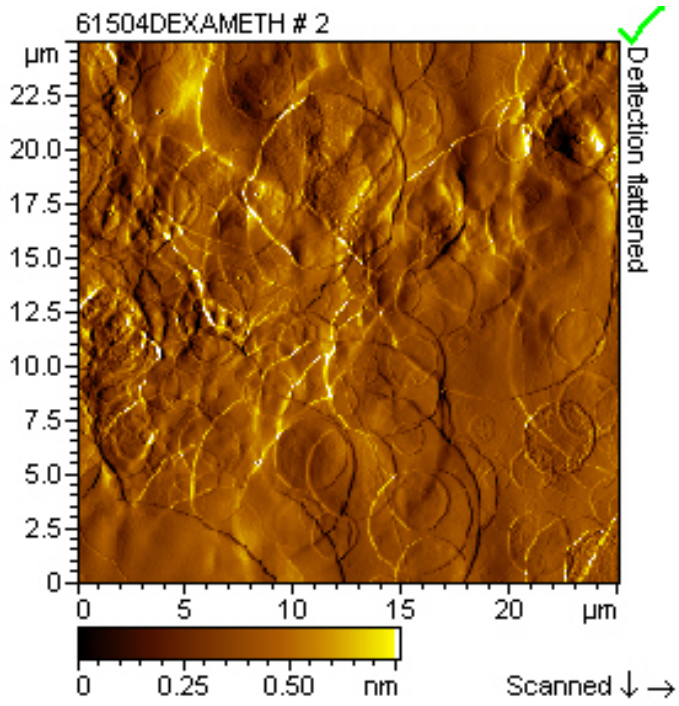

Figure 12. Deflection flattened atomic force micrograph of the MAPLE dexamethasone thin film.

The IR spectra of dexamethasone thin films deposited by MAPLE and drop casting are shown in Figure 13. Dexamethasone deposited by each method revealed three peak absorptions at or near 1720, 1660, and 1620 cm^{-1}. The strong absorption at 1660 cm^{-1} corresponds to the carbonyl group (C=O) seen in the dexamethasone molecule (Figure 6). Correspondence between the two curves indicates that MAPLE deposition did not damage the chemical structure of the drug.

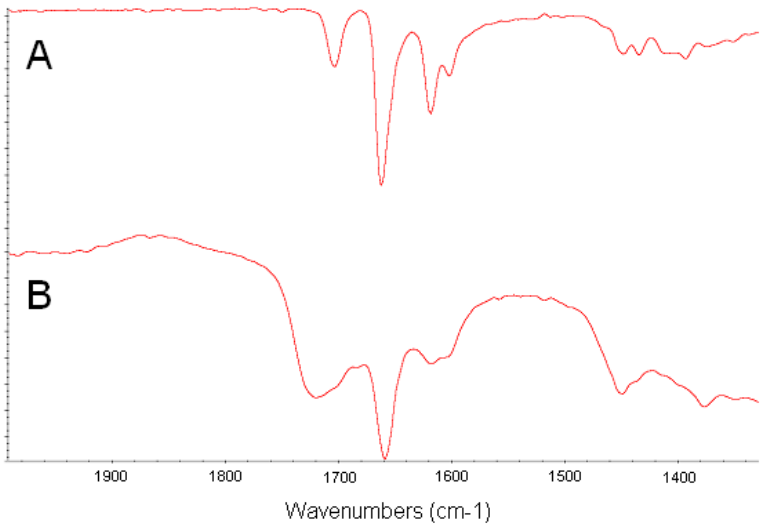

Figure 13. ATR-IR spectra of dexamethasone deposited on Si wafers by (A) drop casting, and (B) MAPLE.

To further examine the effect of the MAPLE process on the bioactivity of dexamethasone, primary microglia were treated with LPS to elicit the inflammatory response of the cells. Microglia were used because they are known to mediate the initial inflammatory response to brain injury for patients undergoing neural electrode insertion. As shown in figure 14, the dexamethasone that was released from the MAPLE-deposited sample effectively inhibited the production of the inflammatory molecule, nitric oxide, by reactive microglia. This result indicates that the dexamethasone was still bioactive following MAPLE deposition.

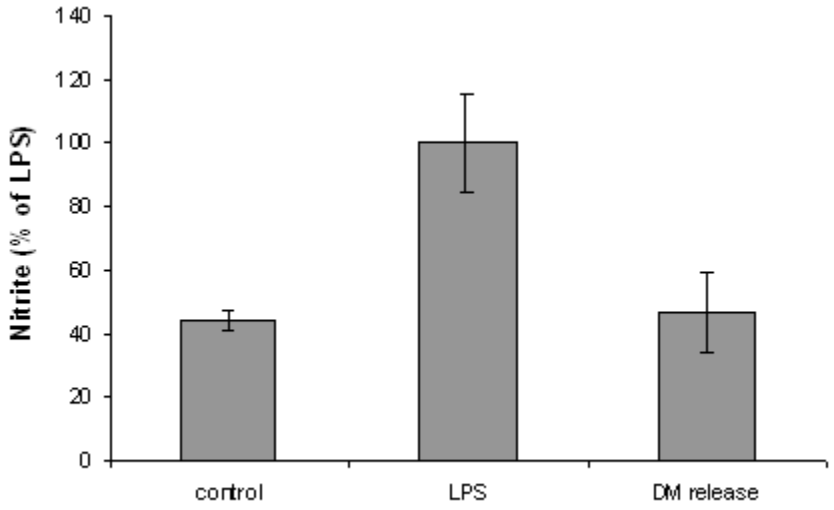

Figure 14. Effect of dexamethasone released from PDLLA/dexamethasone thin films. Microglia were treated with LPS and dexamethasone was released for 48 hours, inhibiting LPS-induced production of nitrite. Cells without LPS treatment served as positive control. Microglia subjected to LPS serum served as a negative control. Data shown are the average ± S.E.M. (n=3). $*P < 0.05$ compared with LPS-treated cultures.

Figure 15 contrasts the drug release profile of MAPLE-deposited dexamethsone thin films and PDLLA/dexamethasone bilayers. In the bare dexamethasone thin film sample, nearly 96% of the drug is released within the first 24 hours. In the PDLLA/dexamethasone bilayer, the dexamethasone release is slowed by 23% as only 73% of the dexamethasone is released in the first 24 hours. Following the initial 24 hours, the PDLLA protective layer prevents the rapid salvation of the dexamethasone layer and prolongs the dexamethasone disassociation. Drug release in the PDLLA/dexamethasone bilayer was seen up to 8 days following sample loading. The sustained release observed over days 2-8 is believed to be attributed to dexamethasone diffusion through the remaining PDLLA matrix.

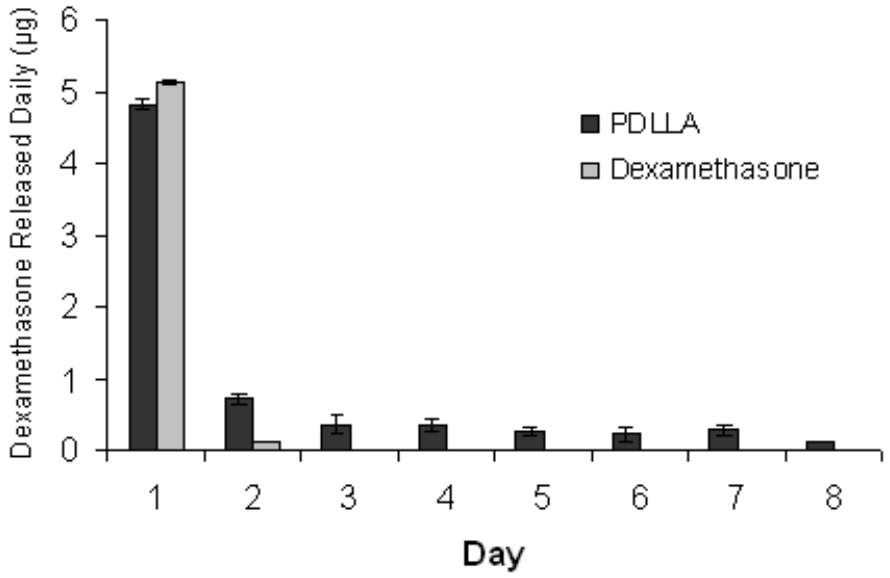

Figure 15. Mass release of dexamethasone from MAPLE deposited PDLLA dexamethasone bilayer. Data shown is average ± S.E.M. (n=3).

The cumulative mass release of dexamethasone from the MAPLE-deposited bilayer is shown in Figure 16. The mass release curve follows a near linear release of dexamethasone between the ranges of 4.9 to 6.7 µg. In an ideal drug-delivery situation, the ideal drug release measure would fall between a range below systemic toxicity and above ineffective dosage. For the MAPLE bilayer system, simply increasing or decreasing the number of laser pulses can vary the amount of drug deposited onto the medical implant. A more delayed dexamethasone release may be achieved by depositing a thicker PDLLA layer onto the dexamethasone monolayer. Using MAPLE, the resulting drug delivery profile (drug quantity and delivery kinetics) can be custom designed by varying the MAPLE deposition parameters.

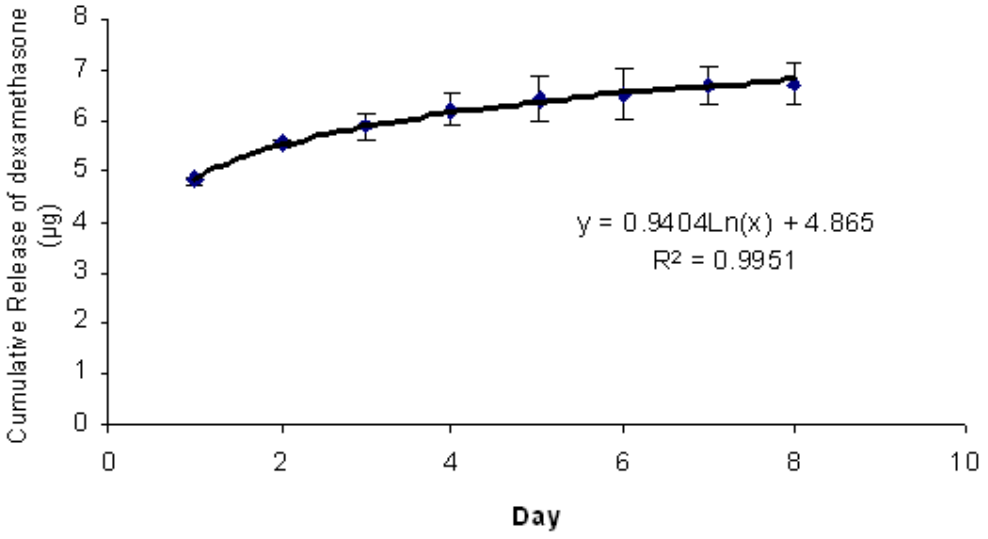

Figure 16. Cumulative mass of dexamethasone released from MAPLE deposited PDLLA-dexamethasone bilayers. Data shown is average ± S.E.M. (n=3). The release profile can be predicted by a logarithmic function at $R^2 = 0.9951$.

Chapter 3. MDW Three-Dimensional Deposition of Neuroblasts

3.1 Introduction

Every year, patients are treated for degenerative or traumatic injury to the peripheral nervous system (PNS) and central nervous system (CNS). Following injury, the adult PNS retains the capacity for regeneration; however, return of motor and sensory function is variable. Repair of the CNS (brain and spinal cord) represents an even greater challenge, because these injuries often lead to an irreversible loss of function. Multiple regeneration obstacles are observed at peripheral nerve lesions, especially at gaps greater than one centimeter in width. Problems including apoptosis, degeneration of the distal stump, swelling of the proximal stump, and gaps between nerve stumps may occur. The autologous nerve graft is the gold standard for treatment of peripheral nerve injury [37]; however, this technique requires invasive graft-harvesting surgeries and offers variable patient outcomes. Current research is focused on developing improved synthetic or hybrid natural-synthetic nerve scaffolds that can be used to guide nerve regeneration across the nerve lesion site. [38] A number of different synthetic materials have been explored for use as nerve guidance channels, including bioresorbable polyesters (e.g., poly(glycolic acid)), [39] bioinert polymers (e.g., polyethylene), [40] and natural materials (e.g., collagen). [41]

Protein gels have been incorporated within nerve guidance channels in order to improve the rate and quality of nerve regeneration. Synthetic conduits filled with Matrigel®, a protein colloid containing collagen type IV, laminin, and glycosaminoglycans, has improved nerve lesion regeneration in adult rats. [40] Growth factor-secreting neuroglial cells have also been incorporated within the lumen of nerve guidance channels in order to improve regeneration. For example, Schwann cells cultured within the lumen of semi-permeable guidance channels have been shown to improve nerve repair in adult rodents. [42] However, little research has been performed on three-dimensionally depositing neurons or other cells within nerve regeneration conduits using direct writing techniques.

Various direct writing techniques including inkjet printing and microstamping have previously been used to pattern neurons onto a two-dimensional substrate. Sanjana and Fuller [43] used an ink-jet printer to fabricate patterns of rat hippocampal neurons and glia on two-dimensional substrates. However, the deposited circular cell patterns were ~200 μm in diameter, and, therefore, do not maintain the precision needed to direct write cells into neural guidance tubes. James et al., [44] used a microstamping technique, whereby poly-l-lysine (PL) is stamped onto two-dimensional electrode arrays and randomly dispersed rat hippocampal neurons preferentially attach to the PL. Microstamping offers better precision than ink-jet printing, but the stamping technique is limited by the un-alterable master stamp pattern. In both cases, neurons were patterned with some precision, but neurons were only patterned on a two-dimensional plane. Overall, these techniques are not capable of three-dimensional cellular deposition nor are they capable of depositing individual cells. Matrix assisted pulsed laser evaporation

direct write (MDW) has the capability to deposit neurons within a three-dimensional hydrogel as well as deposit individual neurons with microscale precision. [45] For this reason, MDW may provide unique capabilities for neuron patterning in nerve regeneration conduits.

Matrix assisted pulsed laser evaporation direct write is a variation of pulsed laser deposition, which is a physical vapor deposition technique commonly used for the deposition of ceramic thin films. A low energy excimer laser ablates a cell-seeded quartz disk, known as a ribbon, according to patterns programmed into computer aided design (CAD) software. The laser energy gently propels cells toward a precise location on the substrate. The resolution of the MDW technique is currently around 10 μm; this value is quite close to the dimensions of many human cells. We have successfully produced patterns of ceramics (e.g., hydroxyapatite) and mammalian cells (e.g., C2Cl2 myoblasts) using this direct writing process. Laser-based direct write processes provide several advantages over solvent-based techniques, including: enhanced cell-substrate adhesion, deposition under ambient conditions, the amount of material transferred can be quantitatively determined, and multilayered structures can be prepared by serial ablation of several ribbons.

Previous experiments using MDW focused on depositing arrays of various cells, including Chinese hamster ovary, [6] embryonal carcinoma, [18] rat cardiac, [1] and human osteoblast cells. [8] In 2004, MDW was first used as a three-dimensional deposition tool. [46] To create a three-dimensional construct, a two-dimensional cellular array was printed onto an extracellular matrix (ECM) substrate, the printed cells were covered with additional ECM and the process was repeated. This process proved

effective and three dimensional patterns were generated. However, this method is labor intensive and maintains the possibility of disruption of the patterned cells though the addition of extra layers of ECM. In our research, we have streamlined this process by direct writing neuroblasts at varying depths directly into the extracellular matrix, which allows for *one step* three-dimensional deposition.

We have demonstrated two- and three-dimensional deposition of B35 neuroblasts using matrix assisted pulsed laser evaporation direct write. The transferred cells were observed with optical and confocal microscopy using TUNEL, α-tubulin, and DAPI nucleic acid immunostains. In these experiments, we examined the following: (1) the ability of MDW to precisely control the penetration depth of neuroblast cells into gelled extracellular matrix, and (2) the behavior of MDW-deposited neuroblasts within the extracellular matrix. This novel cell transfer process may allow for the development of layered, heterogeneous, three-dimensional cell-seeded scaffolds for peripheral nerve repair.

3.2 Materials and Methods

3.2.1 Matrix Assisted Pulsed Laser Evaporation Direct Write

A schematic of the MDW apparatus is shown in Figure 4. The cells to be transferred are immersed within a laser-absorbing matrix and then coated onto a quartz disk. This cell-seeded ribbon is positioned several millimeters away from a receiving substrate. A focused laser pulse is directed at the backside of the ribbon using a UV microscope objective. The laser energy interacts with the cell-seeded matrix at the ribbon/matrix interface, and gently desorbs the matrix from the ribbon. The matrix

assisted pulsed laser evaporation-direct write plume exhibits a front velocity on the order of 100 km/s. A computer program controls the ribbon motion using an XY transition stage. Two-dimensional patterning can be created by lateral and longitudinal movement of both the ribbon and the receiving substrate.

3.2.2 Neuronal Culture and MDW Ribbon Creation

B35 rat neuroblasts (ATCC, Manassas, VA) reproduced rapidly in culture. After reaching 70% confluence in culture, B35 cells were trypsinized and then centrifuged for 5 minutes at 3000 rpm. The resulting cell pellet was collected and resuspended in 1 mL of culture medium (Dulbecco's modified eagle medium (DMEM) supplemented with 10% fetal bovine serum and 1% streptomycin).

The MDW B35 neuroblast-seeded ribbon solution was created by spin coating 200 μL of 1:5 extracellular matrix/DMEM at 1000 rpm for 15 seconds on a 1" quartz disk. The ribbon was then placed in a 37° C incubator for 10 minutes. A 1 mL cell suspension was pipetted onto the ECM/DMEM coated quartz disk, and incubated for 10-15 minutes. The incubated cell-seeded ribbon was then placed on the ribbon holder of the MDW system.

3.2.3 Receiving Substrate

Extracellular matrix (ECM) (ATCC, Manassas, VA) contains a mixture of insoluble basement membrane proteins (e.g., laminin, collagen IV, and fibronectin), proteoglycans, and glycosaminoglycans, which have been shown to support neuronal growth and promote axonal extension. [47-49] In addition, ECM contains several growth factors that assist neuronal growth and proliferation, including TGF-ß, EGF, IGF-1, bFGF, and PDGF. [50]

To prepare the receiving substrate, a 50 μL aliquot of liquid ECM was pipetted onto a 1 cm diameter circular glass slide. For two-dimensional neuroblast transfers, the ECM was polymerized onto the glass slide by incubating the ECM substrate at 37° C for 15 minutes prior to neuroblast transfer. For three-dimensional neuroblast deposition, the ECM coated substrate was exposed to the room temperature for one minute prior to neuroblast transfer.

The receiving substrate was then positioned 700-2000 μm below the neuroblast-seeded ribbon. As illustrated in figure 1, an ArF laser (λ=193 nm, energy density=0.02-0.08 J/cm^2) was focused on the quartz disk; neuroblasts were transferred onto the extracellular matrix substrate in line or rectangle array patterns. Following deposition, the cell-seeded surface was placed in a 37° C incubator for 5-10 minutes in order to allow the ECM to partially polymerize around the embedded neurons. Three milliliters of culture medium was added to the neuroblast-seeded surface. The neuroblast-seeded extracellular matrix substrates were then fixed in 10 % formalin at 24, 72, and 96 hours after cell transfer.

3.2.4 Apoptosis Detection via TUNEL Staining

Apoptosis was detected using a terminal deoxynucleotidyl transferase (TdT)-mediated deoxyuridine triphosphate (dUTP) nickend labeling (TUNEL) kit (Roche, Indianapolis, IN). After the cells had been fixed, they were permeabilized with 0.1% triton at room temperature. The cells were then incubated in the TUNEL reaction mixture for 60 minutes at 37° C. The cell nuclei were next counterstained with DAPI nucleic acid stain (Molecular Probes, Eugene, OR) at 10μM for 5 minutes. The cells were examined using a Nikon E600 fluorescence microscope. If the neuroblasts are apoptotic and

undergoing DNA breakage, the TUNEL staining colors the neuroblast nuclei red. To quantify the number of apoptotic cells, we counted the number of red nuclei compared to blue nuclei (non-apoptotic neuroblasts) at 96 hours post-transfer.

3.2.5 Characterization of Neuronal Morphology in the 3-D ECM Gel

B35 neuroblast morphology was examined using α-tubulin immunofluorescence staining. The fixed samples were washed and incubated in PBS containing 4% goat serum in order to block non-specific binding. Immunostaining of neuroblast cells was performed for one hour at room temperature with mouse monoclonal anti-α-tubulin (Sigma, St. Louis, MO) diluted 1:200. The cells were rinsed in 0.5% triton in PBS, and incubated for an hour at room temperature with goat anti-mouse IgG1 antibody conjugated with Alexa Fluor 488 (Molecular Probes, Eugene, OR) diluted 1:100 with 0.5% triton in PBS.

Cell nuclei were stained by incubating the samples with nuclear 4',6-diamidino-2-phenylindole, dihydrochloride (DAPI, Molecular Probes, Eugene, OR). The samples were mounted on glass microscope slides with Fluoromount-G (Southern Biotechnology Associates, Birmingham, Alabama). The immunostained cells were examined using a Zeiss Axiovert 200M inverted microscope and a Zeiss LSM 510 confocal microscope.

Immunofluorescence staining was also used to measure the number of neuroblast axonal extensions over time. We defined a B35 neuroblast axonal projection as an axon extended greater than one cell diameter. The number of axonal projections were quantified at 24, 48, and 72 hours post-transfer. As a comparative control for the MDW transferred neuroblasts, additional neuroblasts were plated onto a cell culture flasks coated with ECM.

3.2.6 Live/Dead Assay

A live/dead cell staining kit (Biovision, Mountain View, CA) was used to stain the transferred neuroblasts. Neuroblasts were transferred at 0.02 J/cm^2 onto ECM coated quartz disks and staining was performed at 24, 48 and 72 post-transfer. The staining solution was pipetted over the ECM and the solution was allowed to incubate for 15 minutes. Within the solution, the propidium iodide fluoresced dead cells red, and the Live-dye^{TM} stained live nuclei green. The stained neuroblasts were viewed with an inverted optical microscope and a digital still camera with an epi-fluorescence attachment. As a comparative control for the MDW transferred neuroblasts, additional neuroblasts were plated onto a cell culture flasks coated with ECM.

3.3 Results and Discussion

TUNEL staining was performed on the cells 96 hours after laser transfer in order to determine whether the MDW UV-laser transfer process caused neuroblast apoptosis. This staining process can detect cells that have undergone DNA breakage. Only 3% of the transferred neuroblasts were apoptotic. A representative TUNEL staining image is shown in Figure 17 where there are no red nuclei are visible, indicating that no DNA breakage has occurred. Although ultraviolet laser light has the potential to significantly damage DNA bonding, these results suggest that MDW laser transfer does not significantly induce cellular apoptosis. These results further prove previously published reports by Ringeisen et al. that suggest the laser transfer of cells via MDW does not induce apopotosis. [18] Their Comet assay, which measured the amount of cells with single and double strand DNA breakage, showed that pluripotent embryonal carcinoma

cells deposited by MDW did not have significantly more DNA breakage (due to apoptosis) than their control.

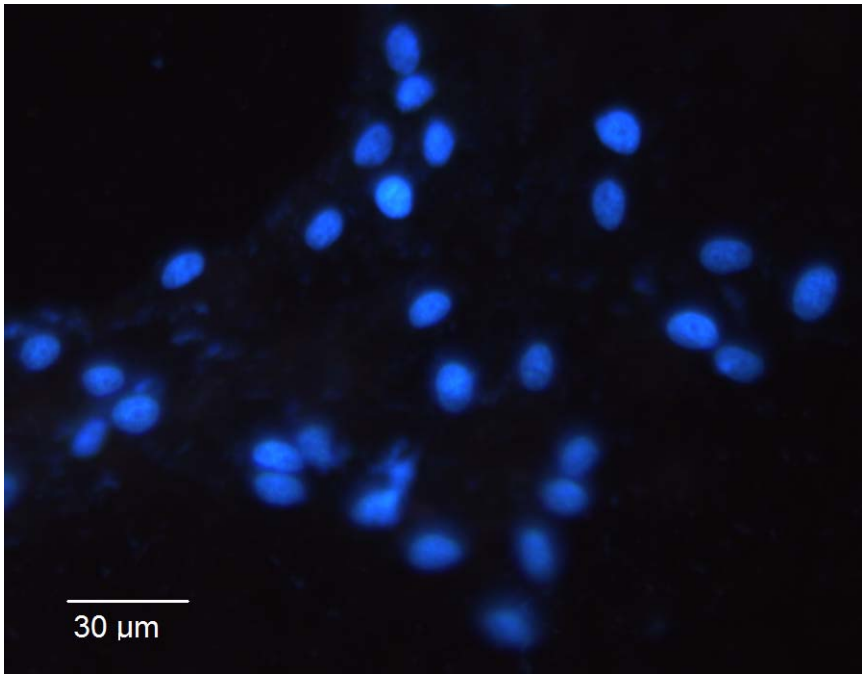

Figure 17. TUNEL staining of transferred B35 neuroblasts. The cells were fixed 96 hours after laser transfer. All cell nuclei counterstained with DAPI nucleic acid stain (blue). No DNA breakage is observed (red).

Figure 18 gives a comparative study of axonal projections of neuroblasts transferred by MDW onto ECM versus neuroblasts cultured on polystyrene culture flasks coated with ECM. In both MDW transferred neuroblasts and the control neuroblasts, the number of axonal projections gradually increased over time with no significant difference between MDW-deposited and control neuroblasts. Similarly, figure 19 reveals the live/dead analysis of neuroblasts transferred by MDW onto ECM versus neuroblasts cultured on polystyrene culture flasks coated with ECM. The percentage of live cells transferred via MDW gradually increased over time while the control remained nearly constant at 100% viable. Over the 72 hours studied, the MDW-transferred neuroblast

population recovered very close (6%) to control levels. In both studies, transferred neuroblasts were transferred using low laser fluence (0.02 J/cm^2).

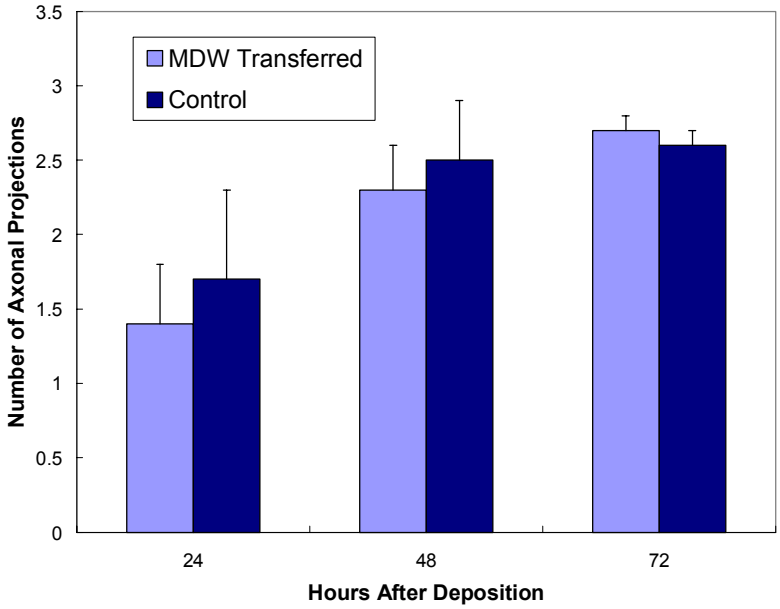

Figure 18. Number of axonal projections over time for MDW-transferred and control neuroblasts. Each bar represents mean $\pm$ STD. Using a students t-test, we found that $p > 0.05$, showing that the MDW transferred neuroblast data was similar to control.

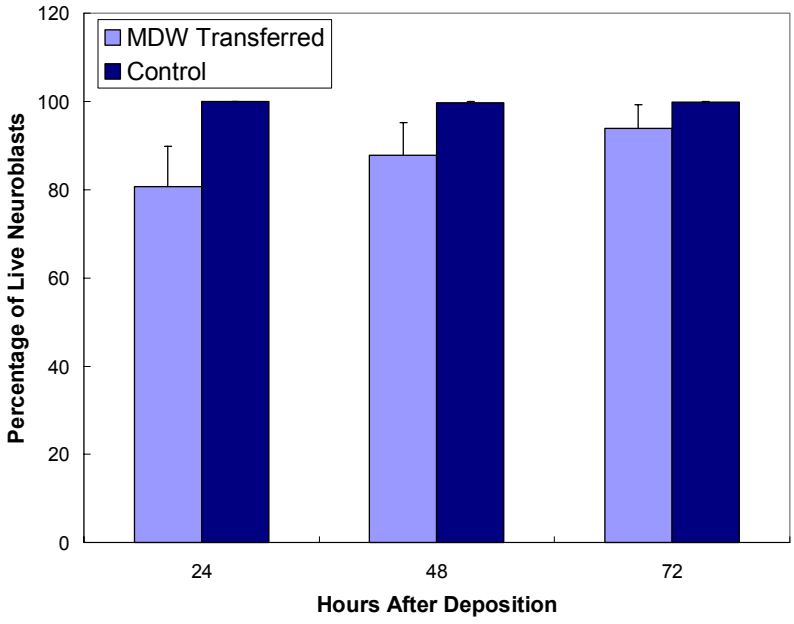

Figure 19. Percentage of live neuroblasts deposited by MDW vs. control. Each bar represents mean $\pm$ STD. Using a students t-test, we found that $p > 0.05$, proving that the MDW transferred neuroblast data was similar to control.

We initially performed two-dimensional cell transfer of B35 neuroblasts to examine the neuroblast morphology after laser transfer. The B35 neuroblasts exhibited a flattened configuration on the ECM surface 24 hours after MDW cell transfer (Figure 20(a)). At that time, the cells began to develop axonal processes within the ECM substrate plane. As indicated by Figure 18, the approximate number of axonal processes for MDW transferred cells was 1.4 +/- 0.4, which is similar to the control neuroblasts (1.7 +/- 0.6). Figure 20(b) depicts the transferred cells 72 hours after deposition. Similarly to the 24 hour samples, the MDW transferred neuroblasts maintained a similar number of axonal projections (2.3 +/- 0.3) as the control (2.5 +/- 0.4). This further proves that the MDW laser transfer of neuroblasts does not significantly impair the neuroblasts ability to produce axonal projections. The transferred neuroblasts appear to have established robust axonal connections. In localized areas, some neuroblasts have formed small two-dimensional networks. Overall, these transfer experiments demonstrate that MDW-transferred B35 neuroblasts create axonal extensions on the polymerized ECM surface in order to form a neuronal network.

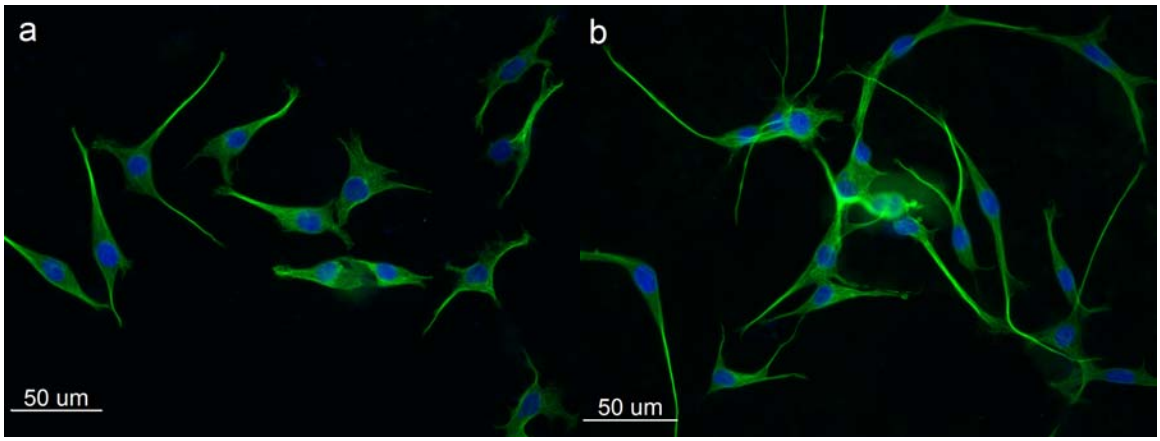

Figure 20. (a) Two-dimensional optical micrograph of B35 neuroblast patterns 24 hours after MDW transfer. The deposited neuroblasts can be seen extending axons over the two-dimensional plane of the extracellular matrix surface. (b) Two-dimensional optical micrograph of B35 neuroblast patterns 72 hours after MDW transfer. The neuroblasts have extended their axons to form local neural networks.

Quartz disks were used to attenuate the incident laser beam prior to interaction with the cell-seeded ribbon; this process allows precise control over laser fluence. At higher laser fluences, the neuroblasts were transferred to greater depths within the extracellular matrix substrate. However, at higher laser fluences, the number of live transferred cells decreases. We found that the percentage of neuroblasts that do not survive transfer quickly increases at fluences larger than 0.08 J/cm^2. Neuroblasts subjected to higher laser energies will either be photolysed or ruptured upon impact with the ECM due to the increased velocity and subsequent stresses. Therefore, we define the depth of penetration maximum as the specific depth to which the transferred neuroblasts are deposited using the maximum safe laser fluence. The depth of penetration maximum value for neuroblasts within gelled ECM was found at 75 μm with an applied fluence of 0.08 J/cm^2.

Figure 21 contains a confocal image of the deposited neuroblasts 75 μm below the surface, which were subjected to a 0.08 J/cm^2 laser fluence. The axonal extensions of B35

neuroblasts transferred to this depth are similar to those observed in neuroblasts transferred in a two-dimensional pattern on the ECM surface (Figure 20). The successful deposition of neuroblasts 75 μm below the ECM allows for the construction of neuroblast-embedded ECM sheets. These polymerized three-dimensional sheets can be stacked on top of each other to form larger three-dimensional structures or can be rolled and can be placed within the lumen of nerve guidance channels.

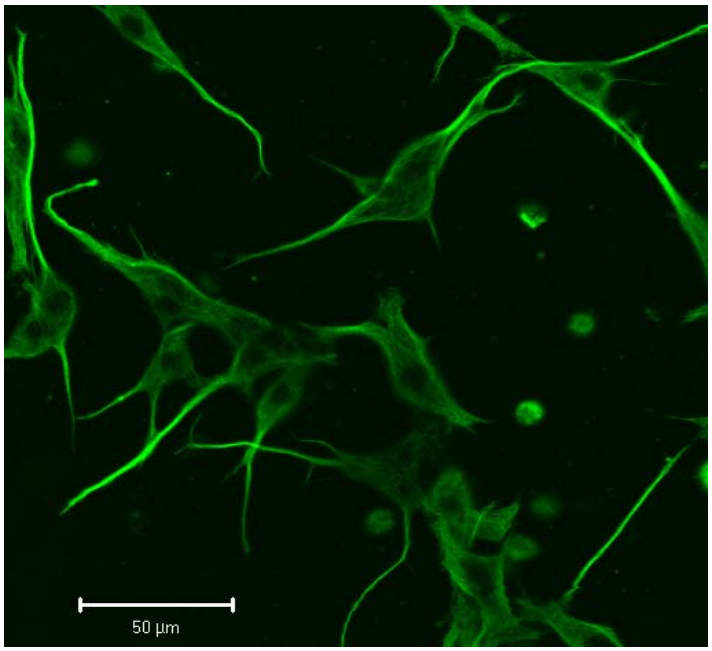

Figure 21. Confocal micrograph of the B35 neuroblasts 75 μm below the extracellular matrix surface 24 hours after MDW transfer. The neuroblasts have extended their axons throughout the three-dimensional ECM network.

B35 neuroblasts were transferred to several depths within an extracellular matrix substrate in order to demonstrate the capabilities of this novel depth-controlled laser transfer process. We initially deposited neuroblasts inside the liquid/gel extracellular matrix using the highest fluence capable of transferring neuroblasts without significantly damaging the neuroblasts (0.08 J/cm^2). A second neuroblast layer was deposited directly on top of this initial level by attenuating the laser beam and lowering the fluence to 0.05

J/cm^2. A third neuroblast array was deposited directly on top of the second array by further attenuating the laser beam and lowering the fluence to 0.02 J/cm^2; this laser fluence transferred cells to the extracellular matrix surface. Figure 22 is a three-dimensional confocal image of this three-dimensional neuroblast array. The laser transferred neuroblasts exhibit axonal extensions within the 0, 45 and 75 μm- deep deposition planes, similar to those observed in two-dimensional neuroblast-seeded scaffolds. In addition, axonal processes have formed between neuroblasts in different deposition planes within the porous extracellular matrix.

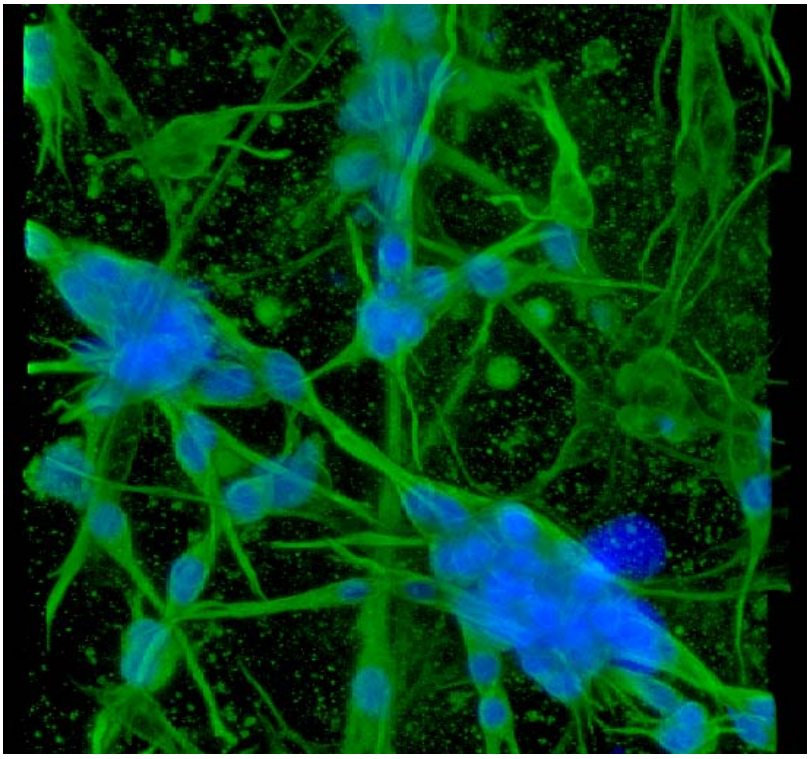

Figure 22. Confocal micrograph of transferred B35 neuroblasts within the extracellular matrix. Axonal extensions were observed between neuroblasts on different deposition planes, which were spaced 30-40 μm apart.

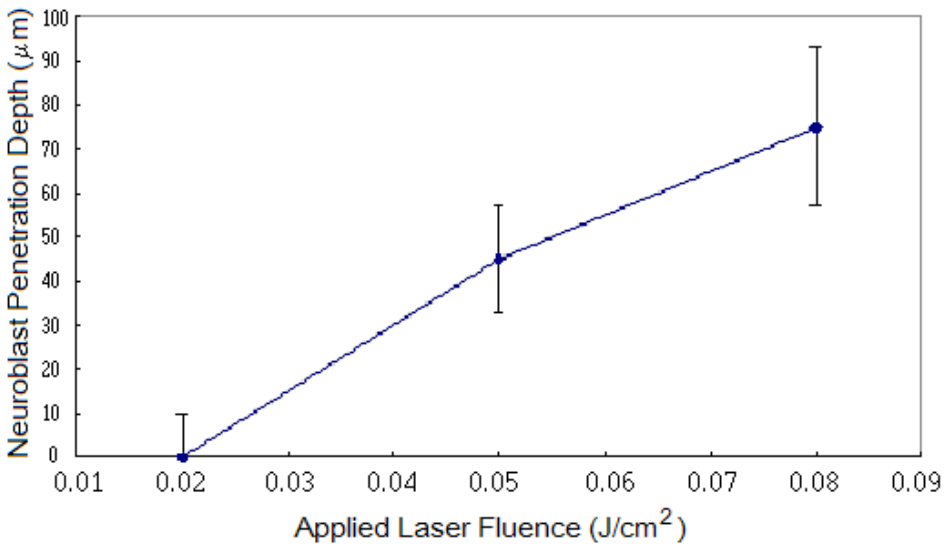

Figure 23. Neuroblast penetration depth (μm) vs. applied laser fluence (J/cm^2). The non-linear effect of applied laser fluence on neuroblast penetration depth is clearly observed.

The penetration of the laser-transferred neuroblast cells within the extracellular matrix substrate is determined by the laser transfer velocity of trypsinized neuroblasts and the viscosity of the extracellular matrix. The physical properties of extracellular matrix have a significant effect on neuroblast penetration depth; ECM is a liquid from –6 to 4 °C system, and spontaneously polymerizes into a gelled stated above that temperature. The viscous force of this Newtonian fluid is proportional to the product of the viscosity and the velocity for a rigid sphere. The value for viscous force is given by Stokes' law as:

$$F = 6 \pi \eta r v \qquad [1]$$

in which r is the radius of the sphere and v is the velocity of the sphere. Figure 23 includes neuroblast depth penetration values measured at three different laser fluences. The non-linear effect of applied laser fluence on neuroblast penetration depth is clearly

observed. Finally, it should be noted that the MDW process exposes the trypsinized neural cells to significant acceleration/deceleration and shear forces. The penetration depth may have a practical limit beyond which acceleration/deceleration and shear will cause cell damage.

Chapter 4. Conclusions and Future Directions

Healthcare consumers continue to demand ever more complex tools for diagnosis and treatment of medical conditions. In the coming decades, implantable sensors, drug delivery devices, and artificial tissues will become significant instruments for medical care. Lasers have demonstrated unique capabilities for thin film processing: direct writing, cutting, and microfabrication of materials used in medical devices. We anticipate that laser processing of microdevices, nanodevices, and tissue engineered materials will be increasingly more significant in the coming years.

There are a wide variety of applications for polymeric and biological thin films in the electronic, microsensor, pharmaceutical and bioengineering industries. Solvent-based coating technologies, such as spin-coating, dip-coating and drop-casting, can result in inhomogeneous films with difficult thickness control. Vapor deposition techniques are too damaging to delicate organic and polymeric materials. Physical vapor deposition techniques, such as sputtering or plasma bombardment have the advantage of controlled layer-by-layer deposition, but they would irreversibly destroy the starting material. MAPLE is a thin film deposition technique capable of depositing a wide array of fragile organic materials without damaging the depositing material or disrupting its chemical structure. MAPLE maintains the attributes of a dry physical vapor deposition technique, such as PVD, but it maintains the fragile material in a solvated state. The MAPLE process deposits a micro-scale smooth thin film, while allowing thickness control by altering the matrix concentration, solvent type, and fluence.

I have explored the use of MAPLE for the deposition of a dexamethasone/PDLLA drug delivery coating for use on medical implants. MAPLE deposited thin films are

superior to films deposited by solvent casting methods because they are free of any residual solvent, which may be harmful to the patient after implantation.

Experimentally, XPS and IR spectroscopy proved that both the PDLLA and dexamethasone thin films were not chemical damaged as compared to a drop cast thin film. AFM revealed that both films maintained micro-scale smoothness with structures averaging only hundreds of nanometers in height. A nitric oxide bioactivity assay ensured that the bioactivity of the dexamethasone was maintained post-transfer. The dexamethasone release from PDLLA/dexamethasone bilayers exhibited a large release over the first 24 hours (73%), which can be attributed to bulk degradation of the PDLLA. The drug-delivery bilayer exhibited diffusion controlled release over days 2-8, before completely exhausting the pharmaceutical.

The PDLLA experiment proved that MAPLE could be utilized as a powerful tool in drug delivery design. MAPLE deposits thin films in a linear fashion, corresponding to the number of applied laser pulses; and, therefore, it can be designed to specifically tailor necessary drug delivery release profiles. Future studies will focus on drug delivery coatings with specific release profiles using different biodegradable polymers and different layering conformations. The successful deposition of these films could lead the way to the development of more sophisticated, multilayer structures. Future multilayer structures could include polymer, drug, growth factor, or antibiotic thin film layers. Depending on the implant application, MAPLE has the capability to deposit any combination of fragile organic materials.

Many direct writing techniques were designed to rapidly construct prototype conformal electronic devices such as interconnects, resistors, and capacitors. Laser

processing techniques such as LIFT and MDW are able to rapidly prototype these devices through ablation or desorption of material from a ribbon, via laser pulses, onto a receiving substrate. Of these two processes, MDW is a gentler method of direct writing because it uses a solvent to desorb the depositing materials from the ribbon. The MDW process has numerous advantages over other controlled deposition techniques, including: CAD/CAM transfer at a rate of 1m/s, transfer under ambient conditions, and 10 μm resolution. The main advantage of MDW is the ability to transfer a wide range of materials including inorganics, organics, polymers, living cells, enzymes, antibodies, and DNA.

We have demonstrated in situ depth-controlled neuroblast transfer within extracellular matrix (ECM) material. Two-dimensional and three-dimensional neuroblast depositions were performed onto and within an extracellular matrix scaffold. Spatial localization of the transferred cells was controlled by varying laser transfer energy and extracellular matrix solidification. By attenuating the laser energy during transfer, we were able to pattern cells at three different depths (0, 45, and 75 μm) below an ECM gel surface. The results obtained indicate that MDW transfer can provide a unique approach for fabricating heterogeneous, layered, three-dimensional cell-seeded scaffolds.

Neuroblasts were used in this experiment in the hope that this process can be applied to construction of seeded ECM lined neural tube conduits. The computer control of the MDW system can theoretically mirror the cellular arrangement of neurons on the injured or severed nerve and help to further guide axons within the tube by forming connections between the severed nerve stumps. We are investigating use of the MDW system to design and fabricate individually tailored cell-seeded scaffolds that precisely

correspond to lesion site geometry. In this way, MDW can be used to treat peripheral nerve injury.

MDW has a large potential for growth in the field of tissue engineering. MDW is capable of depositing tissue scaffold material, living cells and the growth factors needed to induce tissue formation. Combining these techniques could lead to the rapid fabrication of three-dimensional tissue constructs, which would revolutionize the biotechnology, medicine and fundamental cell biology research. MDW has limitless potential and it is only a matter of time before this process is used to rapidly construct individually tailored tissues for wound healing.

References

[1] D. B. Chrisey, A. Pique, R. A. McGill, J. S. Horwitz, B. R. Ringeisen, D. M. Bubb, P. K. Wu, Chem. Rev. 103 (2003) 553.

[2] P.K. Wu, B.R. Ringeisen, J. Callahan, M. Brooks, D.M. Bubb, H.D. Wu, A. Pique, B. Spargo, R.A. McGill, D.B. Chrisey, Thin Solid Films 398 –399 (2001) 607.

[3] R. A. McGill, R. Chung, D.B. Chrisey, P. C. Dorsey, P. Matthews, A. Pique, T. Mlsna, J. Stepnowski, IEEE Trans. Ultrason. Ferroel. Freq. Contr. 45 (1998) 1370.

[4] A. Pique, D. B. Chrisey, B. J. Spargo, M. A. Bucaro, R. W. Vachet, J. H. Callahan, R. A. McGill, D. Leonhardt, T. Mlsna, E. Mater. Res. Soc. Symp. Proc. 526 (1998) 421.

[5] D. M. Bubb, P. K. Wu, J. S. Horwitz, J. H. Callahan, M. Galicia, A. Vertes, R. A. McGill, E. J. Houser, B. R. Ringeisen, D. B. Chrisey, J. Appl. Phys. 91 (2002) 2055.

[6] B. R. Ringeisen, J. Callahan, P. K. Wu, A. Pique, B. Spargo, R. A. McGill, M. Bucaro, H. Kim, D. M. Bubb, and D. B. Chrisey, Langmuir 17 (2001) 3472.

[7] R. Cristescu, D. Mihaiescu, G. Socol, I. Stamatin, I.N. Mihailescu, D.B. Chrisey, Appl. Phys. A 79 (2004) 1023.

[8] P. K. Wu, B. R. Ringeisen, D. B. Krizman, C. G. Frondoza, M. Brooks, D. M. Bubb, R. C. Y. Auyeung, A. Pique, B. Spargo, R. A. McGill, D. B. Chrisey, Rev. Sci. Instr. 74 (2003) 2546.

[9] Z. Kantor, Z. Toth, Appl. Surf. Sci. 86 (1995) 196.

[10] J. Bohandy, B.F.Kim, F.J. Adrian, J, Appl.Phys. 60 (1986) 1538.

[11] Z. Toth, T. Szorenyi, A.L. Toth, Appl. Surf. Sci. 69 (1-4) (1993) 317.

[12] E. Fogarassy, C.Fuchs, F. Kerherve, G. Hauchecorne, J. Perriere. J Appl Phys 66 (1) (1989) 457.

[13] A. Pique, D. B. Chrisey, R. C. Y. Auyeung, J. Fitz-Gerald, H.D. Wu, R. A. McGill, S. Lakeou, P. K. Wu, V. Nguyen, M. Duignan, Appl. Phys. A. Mat. Sci. & Proces. 69 Suppl. S. (1999) S279.

[14] D. B.Chrisey, A. Pique, J. Fitz-Gerald, R. C. Y. Auyeung, R. A. McGill, H. D. Wu, M. Duignan, Appl. Surf. Sci. 154 (2000) 593.

[15] A. Pique, P. Wu, B. Ringeisen, D.M. Bubb, J. S. Melinger, R.A. McGill, D.B. Chrisey. Appl. Surf. Sci. 186 (2002) 408.

[16] A. Pique, R. C. Y. Auyeung, J. L. Stepnowski, D. W. Weir, C. B. Arnold, R. A. McGill, D. B. Chrisey, Surf. & Coat. Tech. 163 (2003) 293.

[17] B. R. Ringeisen, P. K. Wu, H. Kim, A. Pique, R. Y. C. Auyeung, H. D. Young, D. B. Chrisey, D. B. Krizman, Biotechnol. Prog. 18 (2002) 1126.

[18] B. Ringeisen, H. Kim, J. Barron, D. B. Krizman, D. B. Chrisey, S. Jackman, R.Y.C. Auyeung, B. Spargo, Tiss. Eng. 10 (2004) 483.

[19] http://www.epilepsynse.org.uk/ - Statistics from The National Society for Epilepsy (United Kingdom)

[20] Z. Z. Li, R. P. Turner, G. Smith, Epilepsy & Behavior 6(3) (2005) 435.

[21] F. Benedetti, C. Arduino, S. Vighetti, G. Asteggiano, L. Tarenzi, I. Rainero, Pain 111(1-2) (2004) 22.

[22] A. M. Siegel, D. W. Roberts, V. M. Thadani, J. McInerney, B.C. Jobst, P. D. Williamson, Epiliepsia 41(5) (2000) 571.

[23] X. Cui, J. Wiler, M. Dzaman, R.A. Altschuler, D.C. Martin, Biomat. 24 (5) (2003) 777.

[24] A.B. Schwartz, Annu. Rev. Neurosci. 27 (2004) 487.

[25] J.N. Turner, W. Shain, D.H. Szarowski, M. Anderson, S. Martin, M. Isaacson, H. Craighead, Exp. Neurol. 156 (1) (1999) 33.

[26] F. Properzi, R.A.Asher, J.W. Fawcett, Biochem. Soc. Trans. 31 (2003) 335.

[27] B. G. Katzung, A. J. Trevor, Examination & Board Review, Pharmacology, 4th Edition, Appleton & Lange, Norwalk, Connecticut, 1995.

[28] C.M. Liberto, P.J. Albrecht, L.M. Herx, V.W. Yong, S.W. Levison, J. Neurochem. 89 (5) (2004) 1092.

[29] J. McGraw, G.W. Hiebert, J.D. Steeves, J Neurosci. Res. 63 (2) (2001) 109.

[30] J.M. Kim, D. Son, P. Lee, K.J. Lee, H. Kim, S.Y. Kim, J. Pharmacol. Sci. 92 (2003) 74.

[31] S. Golde, A. Coles, J.A. Lindquist, A. Compston, Eur. J. Neurosci. 18 (2003) 2527-2537.

[32] G. Kister, G. Cassanas, M. Vert, Polymer 39(2) (1998) 267.

[33] G. Beamson, D. Briggs (eds.) High Resolution XPS of Organic Polymers, Wiley, New York, 1992.

[34] N. Inagaki, K. Narushima, S.K. Lim, J. Appl. Polym. Sci. 89 (2003) 96.

[35] A. Mayumi, O. Kanie, T. Kitaoka, H. Wariishi, H, J. Fac. Agr., Kyushu Univ. 48 (2003) 97.

[36] W. S. Tsang, C. L. Mak, K. H. Wong, App. Phy. A-Mat Sci. & Proc. 77 (5) (2003) 693.

[37] R. Bellamkonda, P. Aebischer, Biotechnol Bioeng 43 (1994) 543.

[38] C. E. Schmidt, J. B. Leach, Ann Rev Biomed Eng 5 (2003) 293.

[39] H. Molander, Y. Olsson, O. Engkvist, S. Bowald, I. Eriksson, Muscle Nerve 5 (1982); 54.

[40] R. D. Madison, C. F. DaSilva, P. Dikkes, Brain Res 447 (1988); 325.

[41] S. J. Archibald, C. Krarup, J. Shefner, S. T. Li, R. D. Madison, J Comp Neurol 306 (1991) 685.

[42] V. Guenard, N. Kleitman, T. K. Morrissey, R. P. Bunge, P. Aebischer, J Neurosci 12 (1992) 3310.

[43] N. E. Sanjana, S. B. Fuller, J Neurosci Meth 136 (2004) 151.

[44] C. D. James, R. Davis, M. Meyer, A. Turner, S. Turner, G. Withers, L. Kam, G. Banker, H. Craighead, M. Isaacson, J. Turner, W. Shain, IEEE Trans Biomed Eng 47 (2000) 17.

[45] J. A. Barron, B. R. Ringeisen, H. S. Kim, B. J. Spargo, D. B. Chrisey, Thin Solid Films 453-54 (2004) 383.

[46] J. A. Barron, B. J. Spargo, B. R. Ringeisen, Appl Phys A-Mater 79(4-6) (2004) 1027.

[47] R. D. Madison, C. da Silva, P. Dikkes, R. L. Sidman, T. H. Chiu, Exp Neurol 95 (1987) 378.

[48] J. M. Rosen, J. A. Padilla, K. D. Nguyen, M. A. Padilla, E. E. Sabelman, H. N. Pham, Ann Plast Surg 25 (1990) 375.

[49] P. Bovolenta, I. Fernaud-Espinosa, Prog Neurobiol 61 (2000) 113.

[50] E. Falkner, B. Kapeller, H. Eberl, W. Frick, U. M. Losert, K. MacFelda, Int J Artif Organs 26 (2003) 514.